Supplement of

Comparative Nitrogen Speciation in Marine and Coastal Urban Aerosols of the Greater Bay Area and Ecosystem Implications

Cong Cao[1], Wei Chen[2], Xu Yu[2,3], Wing Hei Marco Wong[1], Ningning Sun[4], Kun Zhang[2], Weicong Cheng[5], Jianping Gan[5,6], Jian Zhen Yu[1,2*]

1. Department of Chemistry, Hong Kong University of Science & Technology, Clear Water Bay, Kowloon, Hong Kong, 999077, China

2. Division of Environment and Sustainability, Hong Kong University of Science & Technology, Clear Water Bay, Kowloon, Hong Kong, 999077, China

3. Now at Jiangsu Collaborative Innovation Center of Atmospheric Environment and Equipment Technology, Jiangsu Key Laboratory of Atmospheric Environment Monitoring and Pollution Control, School of Environmental Science and Engineering, Nanjing University of Information Science and Technology, Nanjing, 210044, China

4. Key Lab of Geographic Information Science of the Ministry of Education, School of Geographic Sciences, East China Normal University, Shanghai, 210062, China

5. Department of Ocean Science, Hong Kong University of Science & Technology, Clear Water Bay, Kowloon, Hong Kong, 999077, China

6. Center for Ocean Research in Hong Kong and Macau, Hong Kong University of Science & Technology, Clear Water Bay, Kowloon, Hong Kong, 999077, China

*Corresponding authors. Email: jian.yu@ust.hk

Contents of this file

Section S1. Calculation of $PM_{2.5}$ dry deposition velocity (V_d) for marine and coastal urban environments

To provide a transparent basis for the dry deposition velocities used in the main text, we estimated $PM_{2.5}$ particle dry deposition velocity using the size-segregated particle dry-deposition framework of Zhang et al. (2001). The calculation was performed separately for marine and coastal urban environments. To avoid introducing additional uncertainty from an assumed particle size distribution, a single representative $PM_{2.5}$ dry particle diameter of 0.5 μm and particle density of 1500 kg m^{-3} were used for both environments. The marine and urban surface roughness lengths were set to 2.0×10^{-4} m and 1.0 m, respectively. Neutral atmospheric stability was assumed.

Governing equations

Following Zhang et al. (2001), the particle dry deposition velocity is calculated as

$$V_d = V_g + \frac{1}{R_a + R_s}$$

where V_d is the dry deposition velocity, V_g is the gravitational settling velocity, R_a is the aerodynamic resistance, and R_s is the surface resistance.

(1) The gravitational settling velocity (V_g) is calculated as

$$V_g = \frac{\rho_p d_p^2 g C_c}{18\mu}$$

where ρ_p is particle density, d_p is particle diameter, g is gravitational acceleration, μ is the dynamic viscosity of air, and C_c is the Cunningham slip correction factor:

$$C_c = 1 + \frac{2\lambda}{d_p}\left[1.257 + 0.4\exp\left(-0.55 d_p/\lambda\right)\right]$$

where λ is the mean free path of air molecules.

(2) The aerodynamic resistance (R_a) is calculated as

$$R_a = \frac{\ln(z_R/z_0) - \psi_H}{\kappa u^*}$$

Here, z_R is the reference height, z_0 is the surface roughness length, ψ_H is the stability correction, κ is the von Karman constant, and u^* is the friction velocity. Assuming neutral stability, $\psi_H = 0$, and u^* is estimated from the neutral logarithmic wind profile:

$$u^* = \frac{\kappa U}{\ln(z_R/z_0)}.$$

(3) The surface resistance (R_s) is calculated as

$$R_s = \frac{1}{\varepsilon_0 u^* (E_B + E_{IM} + E_{IN}) R_1},$$

where $\varepsilon_0 = 3$, and E_B, E_{IM}, and E_{IN} are the collection efficiencies by Brownian diffusion, impaction, and interception, respectively. R_1 is the rebound correction factor.

Brownian diffusion is calculated as

$$E_B = Sc^{-c}$$

where c is the land-use-dependent exponent, and Sc is the Schmidt number:

$$Sc = \frac{\nu}{D}$$

$$D = \frac{k_B T C_c}{3\pi\mu d_p}$$

where ν is the kinematic viscosity of air, D is the Brownian diffusivity, k_B is the Boltzmann constant, and T is air temperature.

The impaction efficiency is calculated as

$$E_{IM} = \left(\frac{St}{a + St}\right)^2$$

where St is the Stokes number and a is the land-use-dependent empirical coefficient. For the marine surface, the smooth-surface form is used:

$$St = \frac{V_g u^{*2}}{g\nu}$$

For the urban surface, the collector-radius form is used:

$$St = \frac{V_g u^*}{gA}$$

where A is the characteristic collector radius.

For the urban surface, the interception efficiency is

$$E_{IN} = \frac{1}{2}\left(\frac{d_p}{A}\right)^2$$

For the marine surface, A is not defined for the ocean land-use category, and therefore E_{IN} was set to zero. The rebound correction factor is

$$R_1 = \exp\left(-St^{1/2}\right)$$

The hygroscopic growth equation in Zhang et al. (2001) was not applied in this base calculation because a representative dry particle diameter of 0.5 μm was prescribed. Therefore, the calculated V_d values should be interpreted as dry-particle estimates.

Input parameters

Table S1 summarizes the input parameters used in the calculation. Land-use-dependent parameters were taken from Zhang et al. (2001), with LUC 14 used for the ocean surface and LUC 15 used for the urban surface.

Table S1. Input parameters used for the Zhang et al. (2001)-based $PM_{2.5}$ dry deposition velocity calculation.

Parameter	Marine	Coastal urban	Reference or source
U	5.6 m s^{-1}	2.6 m s^{-1}	Mean wind speed
d_p	0.5 μm	0.5 μm	Zhang et al. (2001)
ρ_p	1500 kg m^{-3}	1500 kg m^{-3}	Qi et al. (2020)
Z_R	10 m	10 m	Approximate 10 m wind reference
Z_0	2×10^{-4} m	1.0 m	Qi et al. (2020); Zhang et al. (2001)
ψ_H	0	0	Neutral stability
κ	0.4	0.4	Constant
k_B	1.38×10^{-23} J K^{-1}	1.38×10^{-23} J K^{-1}	Constant
ε_0	3	3	Zhang et al. (2001)
c	0.5	0.56	Zhang et al. (2001)
a	100	1.5	Zhang et al. (2001)
A	not applicable	0.01 m	Zhang et al. (2001)
T	298.15 K	298.15 K	Representative summer value
P	101325 Pa	101325 Pa	Near sea-level pressure
μ	1.81×10^{-5} kg m^{-1} s^{-1}	1.81×10^{-5} kg m^{-1} s^{-1}	Standard near-surface value
λ	6.65×10^{-8} m	6.65×10^{-8} m	Standard near-surface value

From the prescribed particle diameter and atmospheric constants, the shared particle-related quantities are:

$C_c = 1.336,$

$V_g = 1.508 \times 10^{-5}$ m s^{-1} = 0.00151 cm s^{-1},

$D = 6.448 \times 10^{-11}$ m^2 s^{-1},

$Sc = 2.371 \times 10^5$.

Calculation results

Table S2 summarizes the intermediate variables and final dry deposition velocities for the marine and coastal urban base cases.

Table S2. Calculated intermediate variables and $PM_{2.5}$ dry V_d for the marine and coastal urban base cases.

Variable	Marine	Coastal urban	Unit
u*	0.207	0.452	m s^{-1}
R_a	130.7	12.7	s m^{-1}
E_B	2.05×10^{-3}	9.77×10^{-4}	–
St	4.31×10^{-3}	6.95×10^{-5}	–
E_{IM}	1.86×10^{-9}	2.14×10^{-9}	–
E_{IN}	0	1.25×10^{-9}	–
R_1	0.936	0.992	–
R_s	837.2	761.5	s m^{-1}
V_d	0.11	0.13	cm s^{-1}

Using the Zhang et al. (2001) scheme with a single representative 0.5 μm dry particle, the estimated $PM_{2.5}$ dry deposition velocity was 0.11 cm s^{-1} for the marine environment and 0.13 cm s^{-1} for the coastal urban environment. The urban value is slightly higher than the marine value in this base calculation, despite the lower urban wind speed, because the much larger urban roughness length results in a higher friction velocity and lower aerodynamic resistance. This behavior is consistent with the Zhang et al. (2001) framework, in which fine-particle deposition depends strongly on friction velocity and surface roughness.

These values should be interpreted as first-order dry-particle estimates for a representative 0.5 μm particle. They do not include size-distribution averaging or hygroscopic growth. Because real $PM_{2.5}$-bound nitrogen can be distributed across a range of particle sizes and may undergo hygroscopic growth under humid marine conditions, the effective bulk $PM_{2.5}$ deposition velocity may differ from the single-size estimates reported here.

Table S3. Summary of sampling times, sailing distances, high-NO_x ship-emission notes (exclude from marine samples), and notes on ship stops for the 91 cruise samples.

Sample ID	Date	Start Time	End Time	Duration (h)	Sailing distance (km)	Ship emission influence	Ship stops
AoE01	2024/7/12	10:52:00	12:46:35	1.91	27.6		
AoE02	2024/7/12	15:48:50	20:48:45	2.48	27.7		
AoE03	2024/7/12-13	21:22:50	7:45:10	2.08	22.3		
AoE04	2024/7/13	8:57:40	12:21:30	2.14	22.0		
AoE05	2024/7/13	13:17:20	18:26:55	2.18	21.3		
AoE06	2024/7/13-14	20:15:10	0:02:40	1.88	18.7		
AoE07	2024/7/14	5:48:30	10:04:50	2.24	21.2		
AoE08	2024/7/14	13:12:40	15:46:40	2.57	27.4	✓	
AoE09	2024/7/14	15:53:05	18:18:05	2.42	28.3		
AoE10	2024/7/14	19:36:50	23:34:10	1.89	24.2		
AoE11	2024/7/15	5:30:10	7:39:50	2.16	27.6		
AoE12	2024/7/15	8:41:40	11:39:50	2.97	13.4	✓	
AoE13	2024/7/15	14:05:20	16:10:00	1.72	13.0		
AoE14	2024/7/15	19:11:25	21:25:50	2.24	17.5		
AoE15	2024/7/15-16	21:34:40	7:23:00	9.54	126.5	✓	
AoE16	2024/7/16	10:18:50	15:57:50	5.65	17.1		
AoE17	2024/7/16	16:30:05	19:25:00	2.50	28.8	✓	
AoE18	2024/7/16-17	19:44:45	0:21:10	3.49	30.0		
AoE19	2024/7/17	0:37:20	7:16:30	6.65	0.0		✓
AoE20	2024/7/17	9:14:20	18:56:40	9.71	0.0		✓
AoE21	2024/7/17-18	19:41:50	3:09:00	7.45	0.0		✓
AoE22	2024/7/18	3:27:00	5:59:30	2.54	13.2	✓	
AoE23	2024/7/18	6:34:30	10:20:40	2.94	30.3		
AoE24	2024/7/18	10:51:40	14:22:45	2.58	24.3	✓	
AoE25	2024/7/18	14:46:00	17:20:40	2.28	18.3		
AoE26	2024/7/18	18:42:25	23:16:00	3.46	38.6		
AoE27	2024/7/18-19	23:36:30	5:06:50	4.30	40.6		
AoE28	2024/7/19	5:37:50	9:09:00	2.80	30.8		
AoE29	2024/7/19	9:30:50	12:48:10	2.61	29.4		
AoE30	2024/7/19	13:11:00	16:52:00	2.54	28.6		
AoE31	2024/7/19	18:10:20	20:58:40	2.81	0.0		✓
AoE32	2024/7/19-20	21:12:10	1:43:20	3.11	47.0		
AoE33	2024/7/20	6:21:30	10:16:45	2.57	36.1		
AoE34	2024/7/20	10:37:10	15:07:00	2.48	29.5		
AoE35	2024/7/20	15:49:00	19:19:30	2.52	29.2		
AoE36	2024/7/20	20:15:00	22:53:00	2.09	18.7	✓	
AoE37	2024/7/20-21	23:07:40	3:48:40	3.84	35.6		
AoE38	2024/7/21	4:06:40	7:26:50	2.95	28.8		
AoE39	2024/7/21	7:48:30	11:12:30	2.77	33.9		
AoE40	2024/7/21	11:39:30	15:42:40	3.07	36.2		
AoE41	2024/7/21-22	22:04:20	4:01:00	5.94	0.0		✓
AoE42	2024/7/22	4:21:30	8:20:00	3.02	26.2		
AoE43	2024/7/22	8:49:50	12:19:20	2.53	31.3	✓	
AoE44	2024/7/22	13:04:20	16:40:20	2.44	32.5		
AoE45	2024/7/22	17:31:10	21:29:20	2.43	30.4		
AoE46	2024/7/22-23	22:00:50	4:56:40	6.93	185.2		
AoE47	2024/7/23	5:11:00	9:24:30	4.23	0.0		✓
AoE48	2024/7/23	9:32:10	16:43:40	7.19	0.0		✓
AoE49	2024/7/23-24	16:50:10	0:22:30	7.54	0.0		✓
AoE50	2024/7/24	0:28:30	7:49:10	7.34	0.0		✓
AoE51	2024/7/24	8:10:10	14:11:30	6.02	0.0		✓
AoE52	2024/7/24-25	17:39:10	1:04:30	7.42	0.0		✓
AoE53	2024/7/25	1:10:20	8:28:50	7.31	0.0		✓
AoE54	2024/7/25	8:36:50	10:22:50	1.77	0.0		✓
AoE55	2024/7/25	10:27:00	14:55:10	4.47	49.8		
AoE56	2024/7/25	15:02:50	19:46:20	4.73	0.0		✓
AoE57	2024/7/25-26	19:54:20	12:58:40	17.07	0.0		✓
AoE58	2024/7/26	13:30:00	16:38:40	3.14	0.0	✓	✓
AoE59	2024/7/26	16:45:40	23:19:00	6.56	0.0		✓
AoE60	2024/7/26-27	23:25:30	11:43:10	12.29	0.0		✓
AoE61	2024/7/27	12:32:00	16:01:20	3.38	131.0		
AoE62	2024/7/27-28	17:00:40	5:06:00	12.09	0.0		✓
AoE63	2024/7/28	7:07:00	9:47:40	2.03	22.9		
AoE64	2024/7/28	10:31:10	14:31:00	2.88	36.9	✓	
AoE65	2024/7/28	15:05:40	17:12:50	2.12	27.0		
AoE66	2024/7/28	18:23:50	21:52:10	2.14	28.2	✓	
AoE67	2024/7/28-29	22:20:00	0:26:00	1.58	22.9	✓	
AoE68	2024/7/29	6:05:40	8:40:10	2.03	26.6		
AoE69	2024/7/29	9:18:40	11:57:35	2.08	20.7		
AoE70	2024/7/29	12:39:00	17:22:40	2.84	29.8		
AoE71	2024/7/29	18:20:20	22:49:30	3.18	40.6		
AoE72	2024/7/30	5:43:10	9:57:40	2.44	32.8		
AoE73	2024/7/30	10:46:30	14:24:00	2.41	29.6		
AoE74	2024/7/30	15:03:00	18:48:00	2.24	28.6		
AoE75	2024/7/30	19:09:45	23:37:10	2.68	33.5		
AoE76	2024/7/31	9:45:10	13:00:00	2.22	26.4		
AoE77	2024/7/31	13:20:10	17:19:00	2.31	32.3	✓	
AoE78	2024/7/31	17:51:00	19:47:30	1.86	23.9	✓	
AoE79	2024/7/31	20:29:30	22:34:45	1.46	18.2	✓	
AoE80	2024/8/1	6:36:20	10:22:30	2.58	29.0		
AoE81	2024/8/1	10:52:50	14:36:20	1.92	23.5	✓	
AoE82	2024/8/1	15:16:50	18:50:20	2.53	37.0		
AoE83	2024/8/1	19:20:50	22:38:50	2.33	32.5		
AoE84	2024/8/1-2	22:58:00	0:08:00	1.17	17.5		
AoE85	2024/8/2	5:52:00	8:44:50	1.88	26.3		
AoE86	2024/8/2	9:06:20	11:52:40	2.17	29.4		
AoE87	2024/8/2	12:11:30	14:20:10	1.86	19.9		
AoE88	2024/8/2	14:42:40	19:36:30	4.90	63.4		
AoE89	2024/8/2	20:04:00	21:39:00	1.58	20.5		
AoE90	2024/8/2	22:01:20	23:59:50	1.98	27.9		
AoE91	2024/8/3	6:14:00	10:01:40	3.02	38.4		

Table S4. Statistical comparison of water-soluble $PM_{2.5}$ composition and nitrogen speciation among marine, urban, and ship-emission-influenced samples, using Mann–Whitney–Wilcoxon tests, based on offline AMS measurements. The values in the table represent the one-sided Mann–Whitney–Wilcoxon p values.

Metric	Urban vs. Marine	Ship vs. Marine	Ship vs. Urban	Interpretation
Organics	0.65	0.78	0.97	N.S.
NO_3^-	**4.8×10^{-5}*** **	0.81	0.13	Urban > Marine
SO_4^{2-}	0.63	0.87	0.43	N.S.
NH_4^+	**0.016***	0.57	0.39	Marine > Urban
Cl^-	0.26	0.73	0.64	N.S.
CHN_1	**0.030***	**0.012***	0.13	Urban > Marine, Ship > Marine
$CHN_{>1}$	**0.002****	0.25	0.92	Urban > Marine
$CHON_1$	**0.028***	**0.047***	0.216	Urban > Marine, Ship > Marine
$CHON_{>1}$	0.85	**0.039***	**0.041***	Ship > Urban, Ship > Marine
Amines	0.052	0.09	**0.008***	Ship > Urban
Amides	**0.047***	0.523	**0.022***	Marine > Urban, Ship > Urban
Amino acids	0.22	0.675	0.818	N.S.
Imidazole-like heterocycles	0.19	**0.0026***	**0.0001***	Ship > Marine, Ship > Marine
NO^+/NO_2^+	**0.001****	**0.0081****	0.97	Urban > Marine, Ship > Marine
$C_{\geq 3}$ / ON	**9.4×10^{-8}*** **	**0.0353***	0.11	Urban > Marine, Ship > Marine

Note:
1. N.S. indicates no significant differences among the three sample types.
2. Statistical significance: ***p < 0.001, **p < 0.01, *p < 0.05.
3. All statistical comparisons are based on relative contributions rather than absolute concentrations. Specifically, Organics, NO_3^-, SO_4^{2-}, NH_4^+, and Cl^- represent their mass fractions relative to total water-soluble $PM_{2.5}$; CHN_1, $CHN_{>1}$, $CHON_1$, and $CHON_{>1}$ represent their relative contributions to total ON based on these four categories; and amines, amides, amino acids, and imidazole-like heterocycles represent their relative contributions to total reduced ON, based on the four categories.
4. $C_{\geq 3}$ / ON indicates the N-containing organic fragment signals with carbon number greater than 3 to the total N-containing organic fragment signals.

Figure S1. Photograph of the shipboard aerosol sampling configuration during the cruise campaign. Red boxes and arrows indicate the location of the high-volume air sampler on the upper deck outside the bridge and the nearby NO_x sampling inlet on the lower deck, illustrating their close proximity and the basis for using NO_x as an operational screen for ship-exhaust influence.

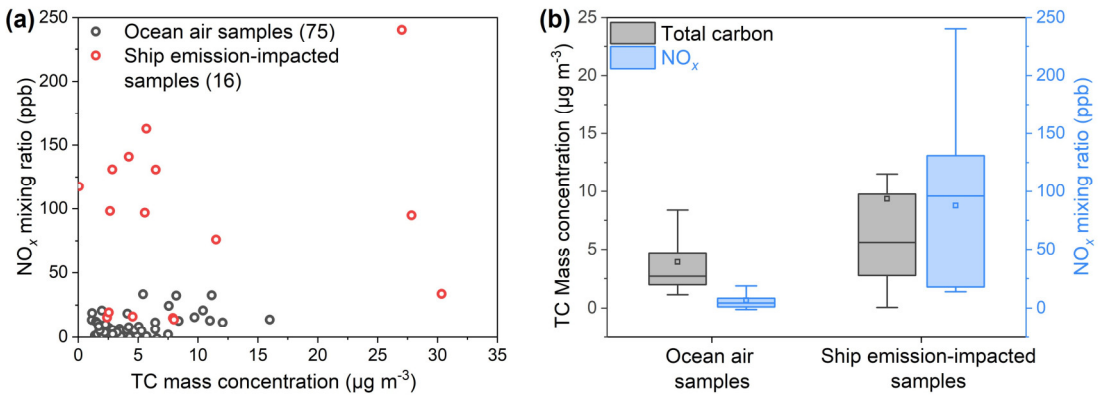

Figure S2. (**a**) Relationship between NO_x mixing ratio (ppb) and TC mass concentrations (μg/m^3). Black symbols denote ocean-air samples (n = 75) used in the subsequent analysis, and red symbols denote ship-emission-impacted samples (n = 16), which were excluded from further analysis. (**b**) Box-and-whisker plots showing TC concentrations (gray boxes, left y-axis) and NO_x mixing ratios (blue boxes, right y-axis) for the ocean-air and ship-emission-impacted sample groups.

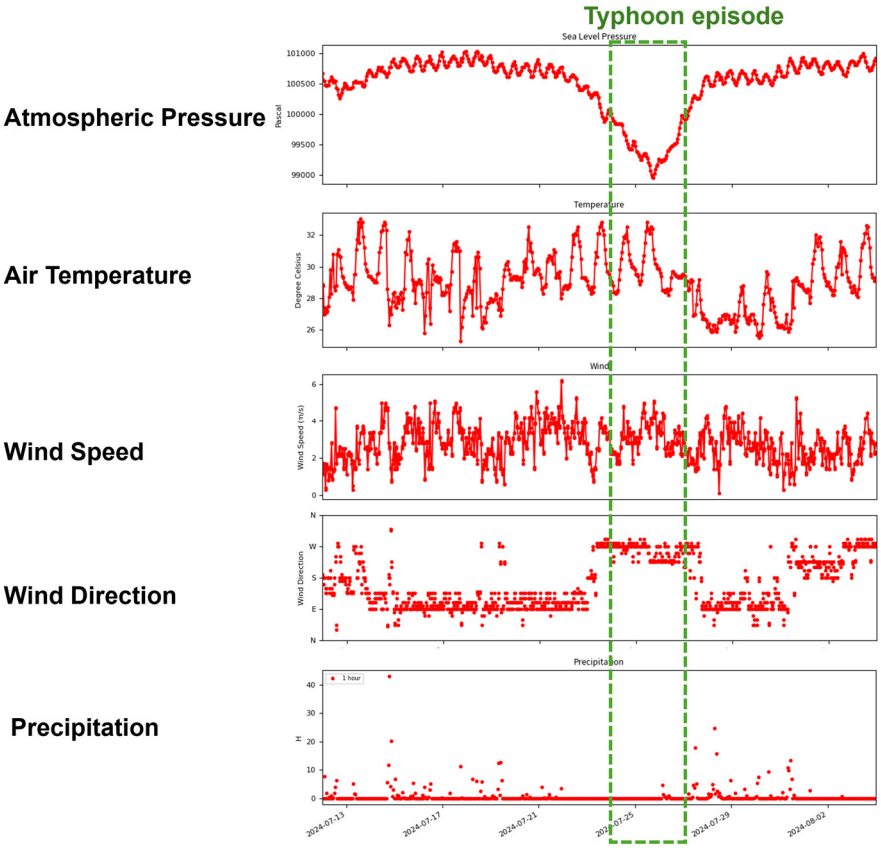

Figure S3. Time series of five key meteorological parameters, including atmospheric pressure, wind speed, wind direction, air temperature, and precipitation, measured at the King's Park station of the Hong Kong Observatory (HKO), located approximately 8 km southeast of the Tsuen Wan (TW) sampling site. The King's Park HKO station represents the closest station to the TW sampling site, with comprehensive observations of meteorological conditions. The green dashed box marks the typhoon-influenced period.

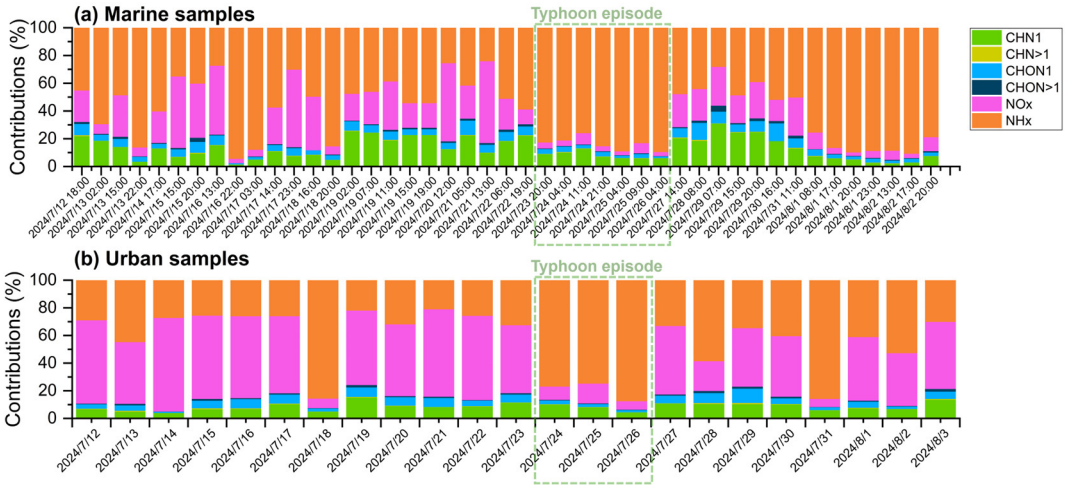

Figure S4. Time series of relative contributions of NH_x, NO_x, and organic nitrogen subgroups (CHN and CHON classes) in marine and urban $PM_{2.5}$, with the typhoon-influenced period highlighted.

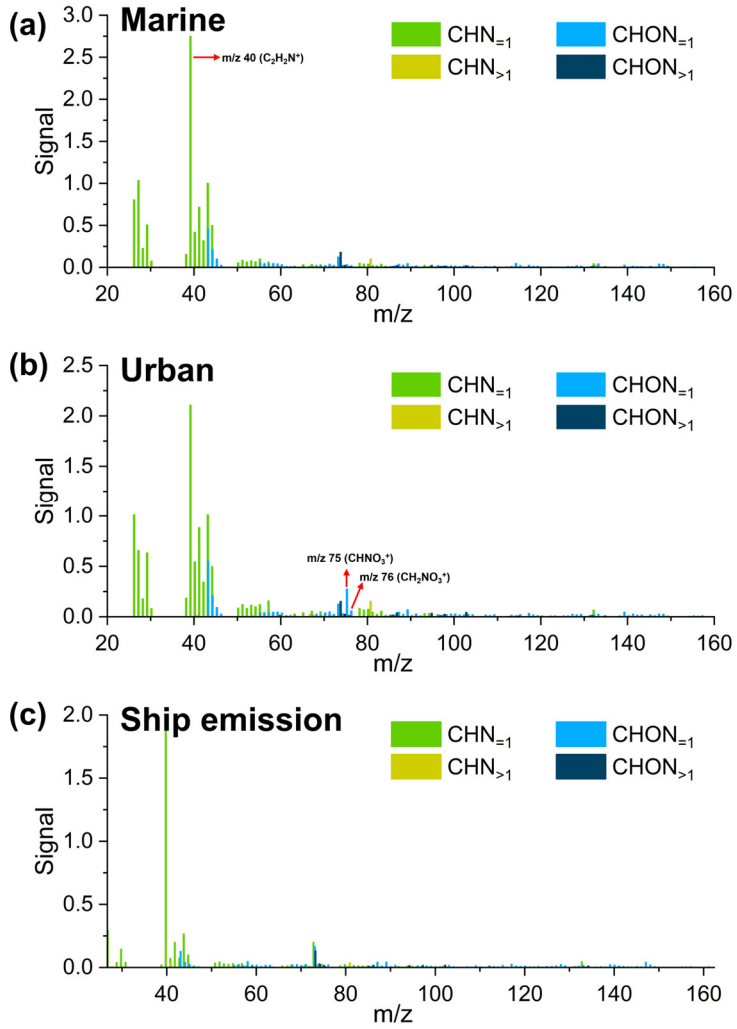

Figure S5. Average nitrogen-containing organic fragments mass spectra for (**a**) marine, (**b**) urban, and (**c**) ship-emission–influenced samples

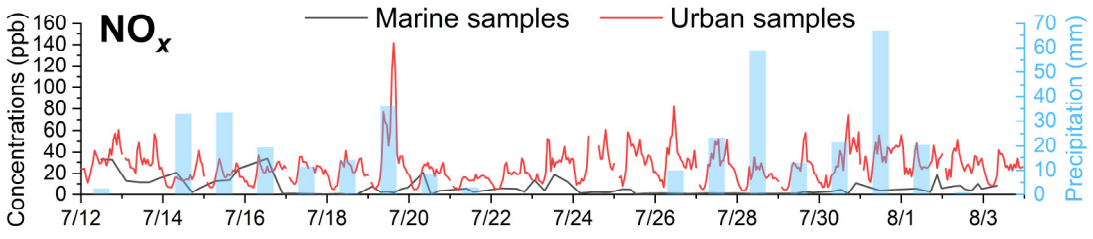

Figure S6. Time series of NO_x concentrations for marine (black line) and urban (red line) samples during the campaign. The urban NO_x data are reported at an hourly resolution, whereas the marine NO_x values are averaged over ~2-hour intervals to match the corresponding filter sampling periods for the marine aerosol samples.

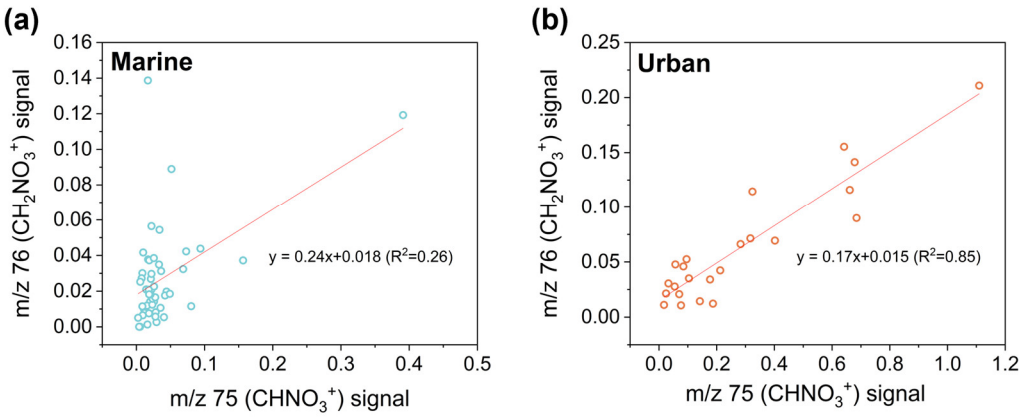

179

180 **Figure S7.** Relationship between $CHNO_3^+$ (m/z 75) and $CH_2NO_3^+$ (m/z 76) signals in (**a**) marine
181 and (**b**) urban samples

182

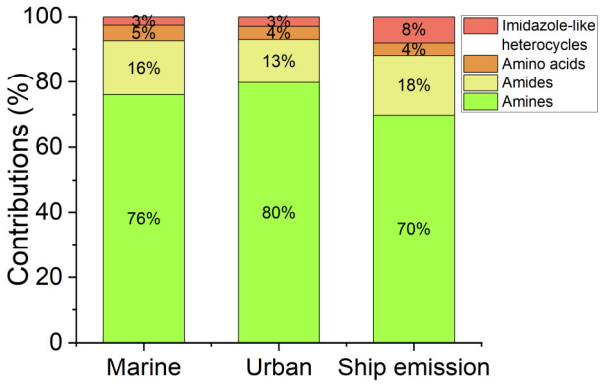

183

184 **Figure S8.** Comparative composition of reduced ON species in marine, urban, and ship-
185 emission-influenced $PM_{2.5}$ samples.

186

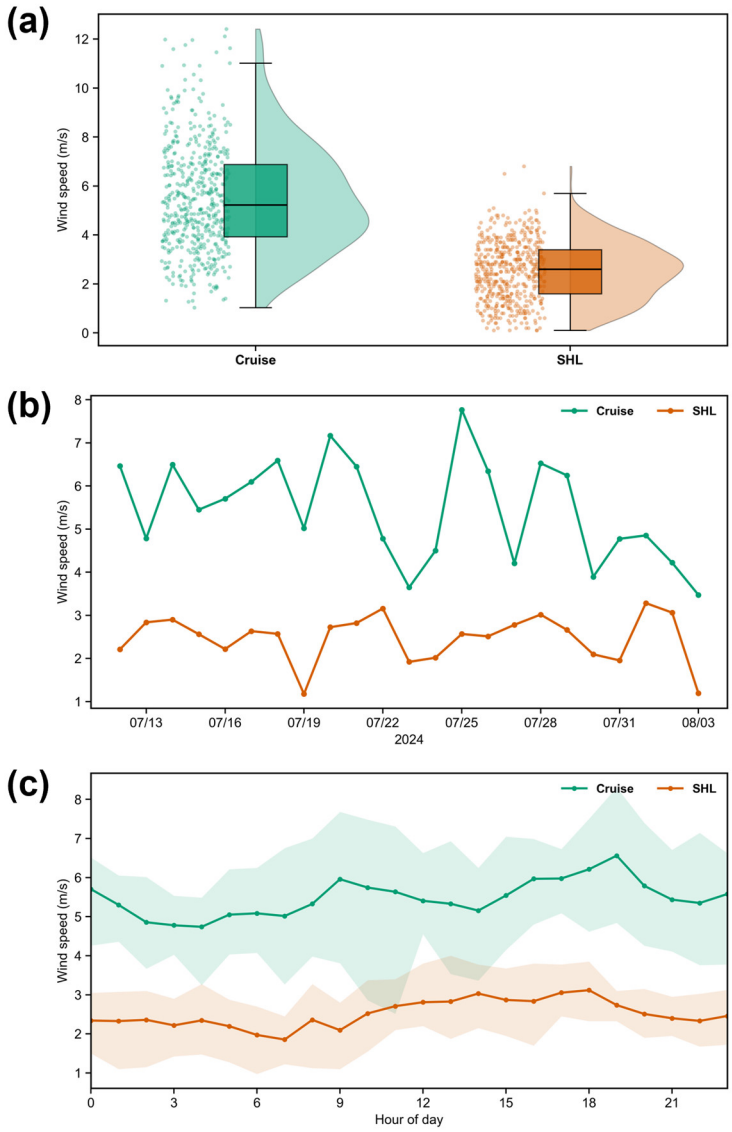

Figure S9. Wind speed comparison between the marine regions (cruise) and the coastal urban site (SHL). (**a**) Box plots of the hourly wind speeds during the campaign period. (**b**) Daily mean wind-speed variations during the campaign period. (**c**) Mean diurnal patterns of wind speed, with shaded areas indicating variability.

Reference

Qi, J., Yu, Y., Yao, X., Gang, Y., & Gao, H. (2020). Dry deposition fluxes of inorganic nitrogen and phosphorus in atmospheric aerosols over the Marginal Seas and Northwest Pacific. *Atmospheric Research*, *245*. https://doi.org/10.1016/j.atmosres.2020.105076

Zhang, L., Gong, S., Padro, J., & Barrie, L. (2001). A size-segregated particle dry deposition scheme for an atmospheric aerosol module. *Atmospheric Environment*, *35*(3), 549-560. https://doi.org/10.1016/S1352-2310(00)00326-5